Results in Chemistry 4 (2022) 100543

Contents lists available at ScienceDirect

Results in Chemistry

journal homepage: www.sciencedirect.com/journal/results-in-chemistry

Experimental and theoretical evaluation of Aspirin as a green corrosion inhibitor for mild steel in acidic medium

Alexander I. Ikeuba [a,b,*], Omang B. John [a], Victoria M. Bassey [a,b], Hitler Louis [b], Augustine U. Agobi [a,b,c], Joseph E. Ntibi [b], Fredrick C. Asogwa [b]

[a] Materials Chemistry Research Group, Department of Pure and Applied Chemistry, University of Calabar, Calabar, Nigeria
[b] Computational and Bio Simulation Research Group, Department of Pure and Applied Chemistry, University of Calabar, Calabar, Nigeria
[c] Department of Physics, University of Calabar, Calabar, Nigeria

ARTICLE INFO

Keywords:
Aspirin
Corrosion inhibitor
Mild steel
Acid corrosion
Adsorption

ABSTRACT

A combined experimental and theoretical approach has been used to evaluate the corrosion inhibition potential of an ecofriendly, cost effective and benign compound (Aspirin) on mild steel in acidic media using hydrogen evolution technique within a temperature range 303 K–333 K in sulphuric acid solution. The results show that Aspirin inhibits the corrosion of mild steel in acidic media. The inhibition efficiency of Aspirin was found to increase with inhibitor concentration and decreased with rise in temperature. The maximum inhibition efficiency was 79.2 % with 800 mg/L of Aspirin at 333 K. The corrosion reaction kinetics in the presence of Aspirin shows a transition from first order to second order kinetics on going on elevating the temperature of the system. The trend in activation energy, E_a and the enthalpy of activation, ΔH indicate that the corrosion process is endothermic, the entropy of activation, ΔS shows that the process is spontaneous. The experimental results were in consonance with Langmuir isotherm and a physical adsorption mechanism is proposed for the adsorption of inhibitor on the mild steel surface. Complementary information was obtained from theoretical computations which show that the E_{HOMO} and E_{LUMO} for Aspirin are −7.33 eV and −2.06 eV, respectively. Molecular dynamics simulation reveals a strong binding affinity between inhibitor and the steel surface with a binding energy of −117.2 kcal/mol at the most stable adsorption configuration.

Introduction

Corrosion is the degradation of a metal or alloy by chemical or electrochemical reaction when it is exposed to the environment. Mild steel, an alloy of iron is widely used various industrial and structural applications due to its appealing thermal and mechanical properties, then again, it is often exposed to harsh environmental conditions which accelerate its rate of degradation [1–4]. Industrial processes such as acid pickling; acid cleaning, acid descaling, and oil-well acidizing are habitually carried out using acids which catalyzes the corrosion processes. In order to mitigate corrosion, many practical methods have been employed which includes the use of inhibitors (including drugs) [5–7], paints, protective coating, and cathodic protection e.t.c. Among all these methods, the use of inhibitors is one of the sustainable approaches of mitigating corrosion [8–10]. Corrosion inhibitors are substances which when introduced into the corrosion environment, decelerates the corrosion rate. Corrosion inhibitors can be obtained from a wide range of organic or inorganic sources which may be synthetic or naturally occurring [11,12]. Most corrosion inhibitors are inorganic or organic molecules which consist of hetero atoms like nitrogen, sulfur, oxygen and pi-electrons in heterocyclic ring systems which are believed to provide sites for adsorption of the molecules on the metal surface. These adsorbed molecules provide a barrier between the metal surface and the corrosive environment [11–13].

Even with the wide use of inhibitors in numerous mild steel industrial applications, toxicity, cost, availability and sustainability remains a persistent issue due to the associated environmental and health challenges, hence, necessitating the urgent need for the development of sustainable environment-friendly, cost effective, non-toxic alternatives [14–17]. There has been recent advances geared towards the reorientation of research focus to the use of benign and environmentally friendly compounds for corrosion protection; otherwise known as green corrosion inhibitors. This captures a wide range of naturally occurring substances and some other synthetic compounds which are mostly

* Corresponding author at: Materials Chemistry Research Group, Department of Pure and Applied Chemistry, University of Calabar, Calabar, Nigeria.
E-mail addresses: ikeubaalexander@unical.edu.ng, ikeubaalexander@yahoo.com (A.I. Ikeuba).

https://doi.org/10.1016/j.rechem.2022.100543
Received 26 June 2022; Accepted 26 September 2022
Available online 27 September 2022

organic in nature including pharmaceutical drugs [18–21].

Research reports reveal that the corrosion inhibition potential of some drugs has been appraised for possible use a competitive class of green corrosion inhibitors. This is because certain drugs meet sustainable environmental requirements for corrosion protection; non-toxic, ecofriendly, readily available and cost effective [13–121]. For instance, the corrosion inhibition performance of gentamicine and sulfamethoxazole [20], domperidone [21], by Ambroxol [22], Cefazolin [23], polyltriazole and [24], penicillin G [25], moxifloxacin [26], 2-Thiophene Acetyl chloride [27], expired ampicillin and flucoxacillin [28], fluconazole [29] have been investigated as green corrosion inhibitor using conventional corrosion monitoring methods such as weight loss, volumetric, thermometric and electrochemical methods [30–33]. In recent times, computational tools have been employed in addition to gain more theoretical insights into the corrosion inhibition mechanism of these inhibitors. For example 2-Thiophene Acetyl Chloride [34], triazole [35], tartaric acid [36], and Imidazoline [37], and isoxazolidine derivatives [38] has been studied using a combined theoretical and experimental approach.

Aspirin (Fig. 1) also known as also known as acetylsalicylic acid is an analgesic, antipyretic and anti-inflammatory drug that comes under the class of non-steroidal drugs. It is a white colored, crystalline compound soluble in alcohols. Aspirin possesses a planar structure with electron-rich oxygen atom and pi electrons [39,40], which favors its possible adsorption capacity, hence, its use as an efficient corrosion inhibitor [41–45].

Aspirin is eco-friendly, readily available, cost effective and a potential compound for corrosion inhibition, however, there is limited information on the temperature-dependent kinetics and thermodynamic parameters of mild steel in the presence of Aspirin which is crucial in predicting the operational lifetime of the metal under service conditions, more also, there is no adequate information on the computational details of Aspirin which is very important in gaining theoretical insights into the elucidation of its corrosion inhibition mechanism. These computational details provide information on quantum mechanical parameters, and molecular dynamics [46–48]. Adequate information on the corrosion inhibition performance of Aspirin will inform key decisions as to its suitability for a possible alternative to the widely applied toxic corrosion inhibitors in the industry. An additional advantage of aspirin over other drugs its facile synthetic route making its application on an industrial scale more practicable.

This work aims to bridge the gap above by adopting a combined theoretical and experimental approach to the investigation of the temperature-dependent kinetics of the corrosion inhibition performance of Aspirin in acidic media. A temperature range of 303–333 K was adopted in an aggressive environment of 1.0 M H_2SO_4. Computational details, thermodynamic and kinetic parameters were deduced and adsorption considerations were made. The results obtained indicate that Aspirin is a promising candidate for the corrosion inhibition of mild steel in acidic media at ambient and elevated temperatures.

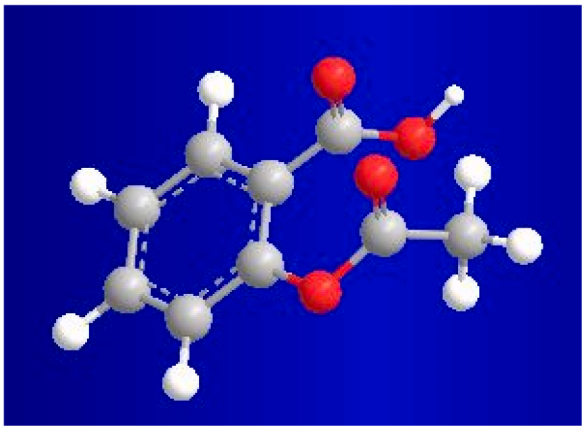

Fig. 1. Molecular structure of Aspirin (Grey, red, and white are C, O and H, respectively). (For interpretation of the references to colour in this figure legend, the reader is referred to the web version of this article.)

Materials and method

Materials

The mild steel sheets used were obtained from the Department of Physics, Mechanical Workshop, University of Calabar. The mild steel composition by weight is: Fe (98.34 %), C (0.08 %), Si (0.26 %), Na (0.64 %), S (0.05 %), Ni (0.09 %),Cr (0.08 %), Mn (0.02 %) and Cu (0.27 %). The steel sheet was mechanically press cut into 2 cm × 5 cm coupons with thickness of 0.08 cm. The samples were abraded with different grades of emery paper from 600 to 1000 grit, degreased in ethanol, dried in acetone, and stored in a moisture free desiccator. The corrosive medium was 1.0 M H_2SO_4 prepared with analytical grade reagents supplied by Sigma – Aldrich. Distilled water was used for the preparation of all the reagents. All weighing was done with AEADAMPGW253e digital analytical balance [14,15].

Sample characterization

Aspirin was characterized by Fourier-transform infrared spectroscopy (FTIR) within the wavelength range of 400–4000 cm^{-1} using a IS50 FT-IR, Thermo Scientific, Waltham, MA, USA. The 1H NMR spectrum was recorded using a Bruker Avance III 600 MHz spectrometer (Bruker). The mild steel surface morphology and chemical composition were analyzed using XL30 type ESEM SEM coupled to EDX.

Preparation of stock solution of Aspirin

Aspirin tablets were ground to powder; 400 mg of the powder was weighed and dissolved in 500 mL of the blank solution (1 M H_2SO_4) to get 800 mg/L concentration. The stock solution of 800 mg/L was serially diluted to get 50 mg/L, 100 mg/L, 200 mg/L, and 400 mg/L. These solutions were then used for the corrosion test at temperatures of 303 K, 313 K, 323 K and 333 K using the gasometric assembly.

Gasometric method

The reaction flask was filled with 100 mL blank solution of the corrodent connected to a burette through a delivery tube. A weighed mild steel coupon was dropped into the solution in the air tight flask, and the reaction vessel was quickly closed to avoid any escape of hydrogen gas. The volume of the hydrogen gas evolved from the reaction was monitored by the depression in the level of paraffin oil in the burette. This depression in the paraffin oil level was recorded every minute for 30 min at 303 K, 313 K, 323 K and 333 K. The same experiment was repeated in the presence of the Aspirin at concentrations of 50 mg/L, 100 mg/L, 200 mg/L, 400 mg/L and 800 mg/L. The rate for the hydrogen evolution was obtained from the slope of the trend line of the graph of volume of hydrogen evolved against time [16].

Computational details

Geometry optimization of Aspirin was performed using density functional theory with the Yang- Parr non local feature vector (B3LYP) and 6–31 + G(d,p) basis set. Complete molecular structure simulation together with the vibrational analysis of Aspirin was carried out using the Gaussian 09 software kit. Frontier molecular orbital (HOMO or LUMO) analysis were carried out from which important quantum parameters were calculated such as ionization potential *(I),* electron affinity *(A),* absolute electronegativity *(X),* absolute Hardness (η), and Softness (σ). The adsorption of Aspirin on the mild steel was simulated

using the Material Studio software's adsorption locator module where COMPASS is used for force field approximations.

Results and discussion

Structure confirmation of Aspirin

Fourier transform-Infrared (FT-IR) analysis

FT-IR spectrum of Aspirin was obtained theoretically and experimentally to confirm its identity. The theoretical and experimental FT-IR spectrums of Aspirin are shown in Fig. 2a and b, respectively. Peaks were observed for different functional groups which correspond to [–OH, C—H and C—O] which confirmed the presence of these functional groups in Aspirin. The theoretical and experimental values of FT-IR are shown in Table 1. The characteristic region for the aromatic rings is between 3300 and 3000 cm^{-1} [49]. Aspirin C—H stretching vibration were observed at 3187.7 cm^{-1} experimentally and calculated to be 3193.2 cm^{-1} theoretically which is consistent with values reported elsewhere in the literatures [50]. It is observed from the potential energy distribution (PED) analysis that the entire vibrational mode mentioned are pure C—H stretching because of the PED percent which is 99 %. The rings O—H stretching vibration generally appear in the spectrum as a sharp peak between 3650 and 3600 cm^{-1}. This band appears in combination with the hydrogen bonded O—H peak when the alcohol is dissolved in a solvent. Aspirin O—H stretching vibration are calculated to be 3649.5 cm^{-1} experimentally and 3634.4 cm^{-1} theoretically which corresponds to values elsewhere in literature [49–54]. It is observed from the PED analysis that the entire vibrational mode mentioned are pure C—H stretching because of the PED percent which is 100 %. Aspirin gives stretching bands in the region 1300–1000 cm^{-1}. Aspirin O—H stretching vibration are calculated to be 1286.4 cm^{-1} experimentally and 1281.5 cm^{-1} theoretically which corresponds to other theoretical values from literature. It is observed from the PED analysis that the entire vibrational mode mentioned are pure C—H stretching because of the PED percent which is 61 % [52,53].

Nuclear magnetic resonance (NMR) analysis

^{1}H NMR is an important spectroscopic technique for the identification of molecular structure and presence of different proton environment. The 1H spectra of aspirin were recorded using deuterated methanol as solvent and TMS as internal standard reference. The experimental and theoretical 1H NMR spectra are shown in Fig. 3 and the chemical shifts are shown in Table 2. The 1H NMR spectrum shows six distinct proton signals which indicates that the Aspirin compound has six different proton environments. The proton signal at δ 2.39 is attributed to CH_3 protons of Aspirin moiety. The next four signals in the downfield region at δ 7.65, δ 7.85, δ 7.90, δ 8.15 are due to the C5, C3, C4 and C6 benzene ring protons. The last signal further downfield at 9.20 δ is attributed to OH hydroxyl protons of Aspirin. The deviation between experimental and theoretical chemical shift observations is low suggesting the close conformity of experiments with theory [15].

Table 1
Theoretical and experimental values of FT-IR wavenumbers of Aspirin.

Experimental (cm^{-1})	Theoretical (cm^{-1})	Assignment with PED (%)
3187.7	3193.2	νCH(99)
3649.5	3634.4	νOH(1 0 0)
1286.4	1281.5	νOC(61)

Corrosion inhibition Evaluation: Hydrogen evolution experiment

The acid corrosion of mild steel is characterized by evolution of hydrogen and the rate of hydrogen evolved is directly proportional to the corrosion rate [16,17]. The volume of hydrogen evolved during the corrosion of mild steel in 1 M H_2SO_4 solution in the presence and absence of Aspirin at 303 K, 313 K, 323 K and 333 K, was measured as a function of time. The results obtained are depicted in Figs. 3-6. The volume of hydrogen evolved was observed to decrease in the presence of Aspirin compared to that of the blank solution. The corrosion rate was obtained from the slope of the trend line of the graph of hydrogen per unit area versus time. From the values of the corrosion rate, the surface coverage and inhibition efficiency were then calculated using equation (1) and (2). The calculated corrosion rate, surface coverage and inhibition efficiency are presented in Table 3.

$$\theta = 1 - \frac{C_{R(inh)}}{C_{R(Blank)}} \quad (1)$$

$$IE = \theta \times 100 \quad (2)$$

where C_R is the corrosion rate, θ is the surface coverage, IE (%) is the inhibition efficiency, $CR_{(inh)}$ and $CR_{(Blank)}$ are the rates of hydrogen evolution in the presence and absence of Aspirin, respectively.

Effect of concentration of Aspirin on corrosion of mild steel

The effect of Aspirin concentration on the corrosion of mild steel in acidic media was studied by varying the concentration from 0 mg/L (blank) to 800 mg/L. The volume of hydrogen evolved with time for the corrosion of mild steel in 1 M H_2SO_4 in the presence and absence of inhibitor of different concentration blank, 50 mg/L, 100 mg/L, 200 mg/

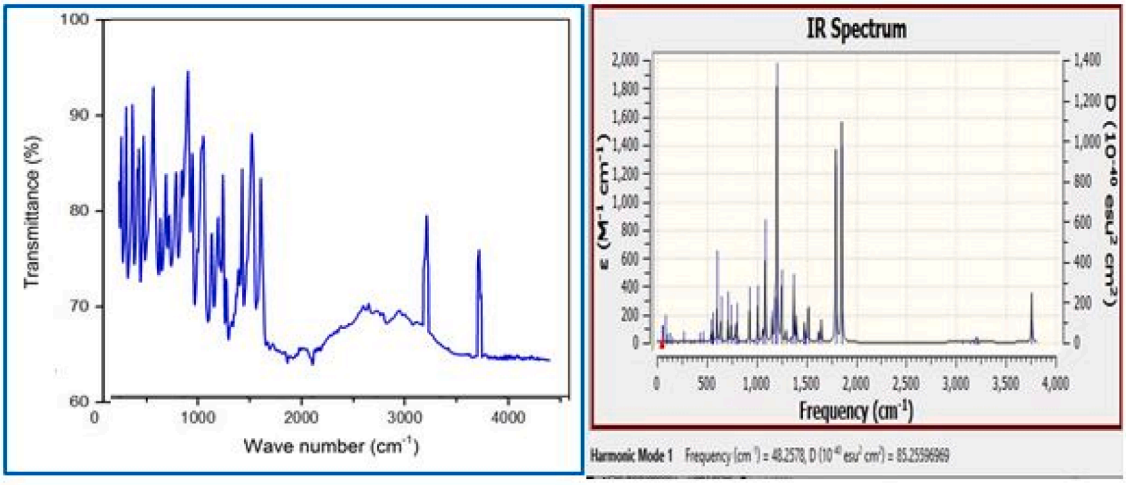

Fig. 2. IR spectrum of Aspirin (a) Experimental (b) Theoretical.

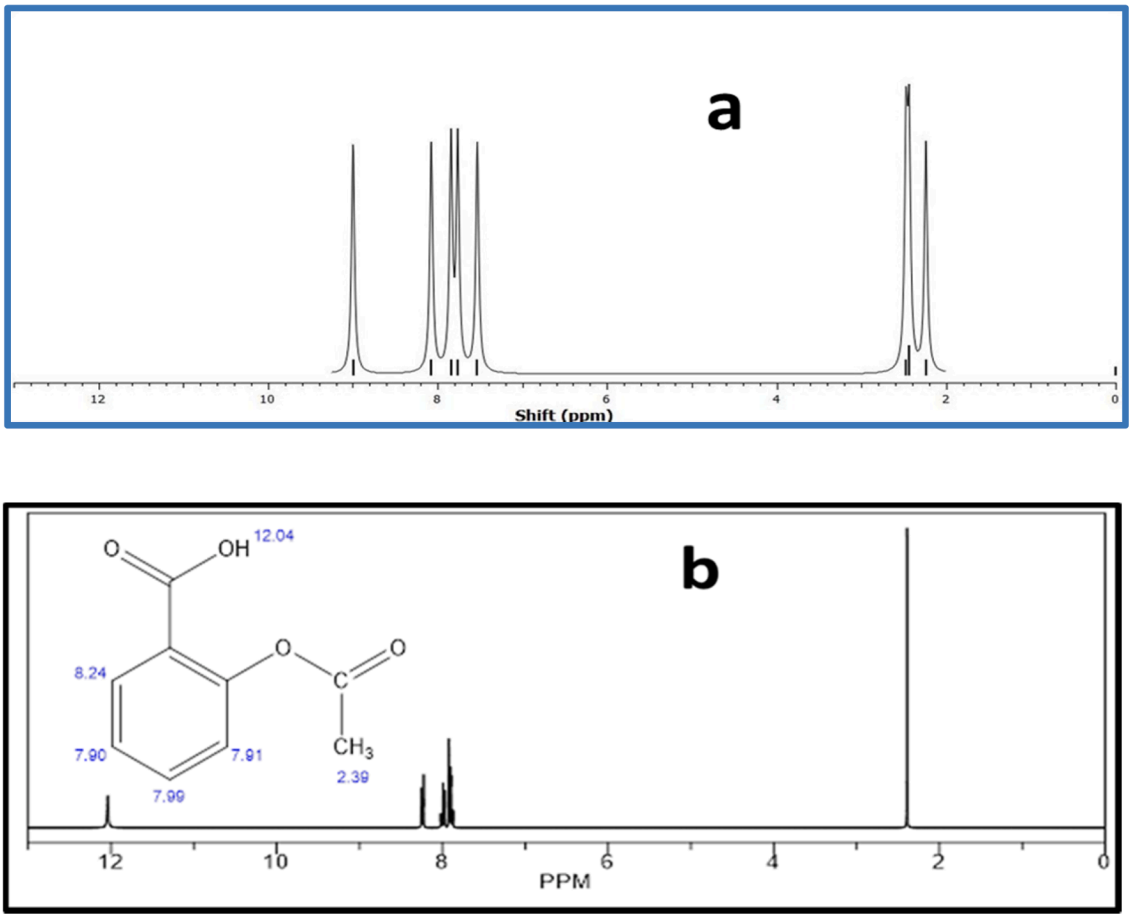

Fig. 3. NMR spectrum of Aspirin (a) Experimental (b) Theoretical.

Table 2
^{1}H NMR Experimental and theoretical values of chemical shifts (δ) of Aspirin.

S/N	Experimental (ppm)	Theoretical (ppm)	Assignment
1	2.40	2.39	CH_3 methyl protons
2	7.85	7.91	C3 benzene ring protons
3	7.90	7.99	C4 benzene ring protons
4	7.65	7.90	C5 benzene ring protons
5	8.15	8.24	C6 benzene ring protons
6	9.20	12.04	OH hydroxyl proton

L, 400 mg/L and 800 mg/L of Aspirin at a temperature of range 303 K – 333 K which are shown in Figs. 4-7. The calculated corrosion rate, surface coverage and inhibition efficiency are presented in Table 3. It is observed that on addition of Aspirin, the corrosion rate decreased compared to that of the free solution (blank). This indicates that the presence of Aspirin lowers the corrosion rate of mild steel in acidic media. The volume of hydrogen evolved and the corrosion rate is seen to decrease with increase in the concentration of the Aspirin across 303 K – 333 K (Figs. 4-7 and Table 3). The surface coverage and percentage inhibition efficiency increases with increase in Aspirin concentration which is consistent with the general observation for typical corrosion inhibitors [19–25]. This trend of the effect of concentration of Aspirin on the corrosion of mild steel was similar across the temperatures studied. The maximum inhibition efficiency were all obtained at 303 K for 50 mg/L, 100 mg/L, 200 mg/L, 400 mg/L and 800 mg/L of Aspirin; 26.9 %, 53.6 %, 64.1, 71.2 % and 79.2 %, respectively. This increase in inhibition efficiency with concentration is attributed to the increase in the fractional surface coverage, θ (i.e. the fraction of the metal surface covered by the aspirin molecules). It is widely reported with experimental evidence that the inhibitory action of inhibitor molecules is predominantly by adsorption of the molecules on the metal surface thereby creating a protective barrier film on the metal surface, hence reducing the corrosion rate of the substrate [19–25].

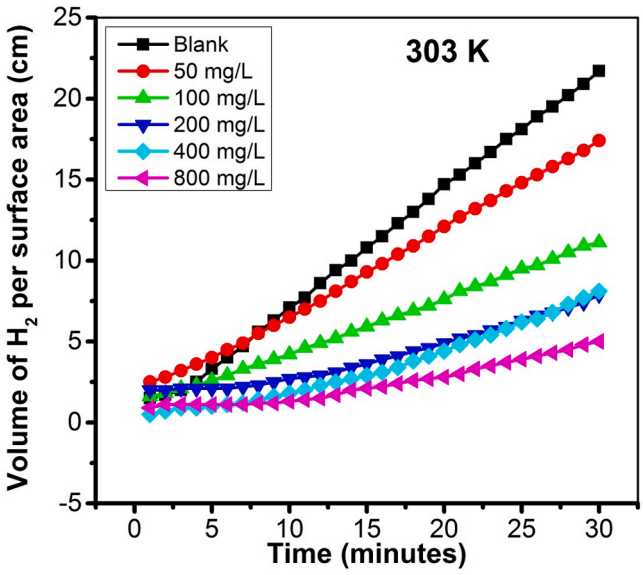

Fig. 4. Variation of volume of hydrogen evolved (V_H) with time for the mild steel coupons in 1 M H_2SO_4 solutions containing Aspirin at 303 K.

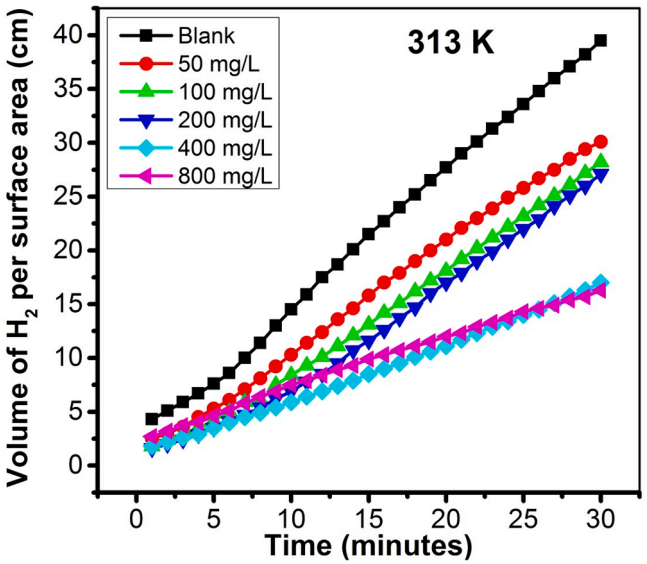

Fig. 5. Variation of volume of hydrogen evolved (V_H) with time for the mild steel coupons in 1 M H_2SO_4 solutions containing Aspirin at 313 K.

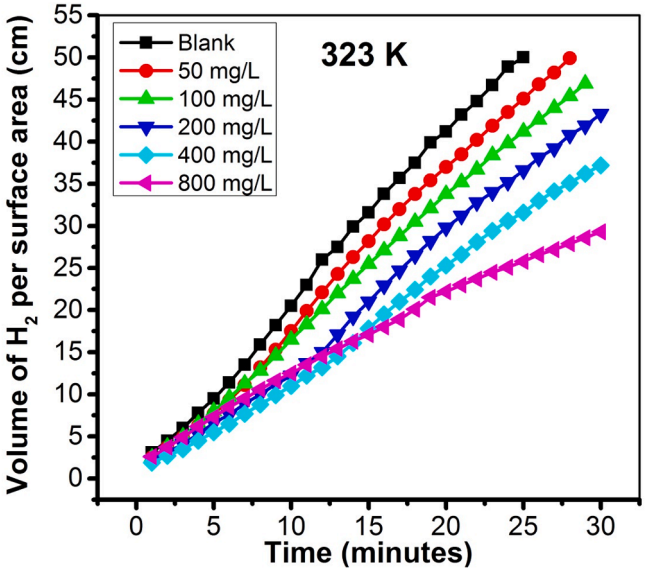

Fig. 6. Variation of volume of hydrogen evolved (V_H) with time for the mild steel coupons in 1 M H_2SO_4 solutions containing Aspirin at 323 K.

Effect of temperature on corrosion mild steel in the absence and presence of Aspirin

The effect of temperature on corrosion inhibition of Aspirin on mild steel in 1 M H_2SO_4 was monitored in the absence and presence of Aspirin across the temperature range 303 K – 333 K. The effect of temperature on the rate of corrosion of mild steel can be seen from Table 3. The corrosion rate is observed to increase with an increase in temperature; this probably can be due to the expected increase in chemical dissolution of mild steel with rise in temperature [17,18]. The surface coverage and inhibition efficiency is seen to decrease with a rise in temperature, suggests a decrease in the potency of Aspirin to inhibit mild steel corrosion at elevated temperatures. This suggests a physical interaction between the Aspirin molecules and the mild steel surface. Probably physisorption of Aspirin may likely be the predominant phenomena at the metal surface, this is speculated because of possible desorption of adsorbed Aspirin from the metal surface at elevated temperatures due to increased agitation of solution which is capable of shaking off weakly adsorbed Aspirin molecules. The maximum inhibition efficiency at obtained at 303 K, 313 K, 323 K and 333 K are 79.2 %, 62.9 %, 55.1 % and 46.1 %, respectively at 800 mg/L of Aspirin. The In order to determine the nature of the interaction of Aspirin and the mild steel surface, the experimental data were further subjected to further thermodynamic analysis and tested further using different adsorption isotherms.

Morphological changes in the mild steel surface before and after treatment with Aspirin

Figurrre 8a-c show the SEM surface morphologies of mild steel sheets before and after exposure to 1 M H_2SO_4 solution in the presence and absence of 800 mg/L Aspirin after 1 h at 303 K. Fig. 8a is the SEM image of the polished mild steel surface which shows a smooth and clean surface. Fig. 8b is the mild steel surfaces in 1 M H_2SO_4 the absence of Aspirin, the image shows a roughly damaged surface indicating the rapid degradation of mild steel. Fig. 8c is the mild steel surface in the presence of 800 mg/L in 1 M H_2SO_4, the image shows a relatively uniform surface with an insignificant corrosion activity. Fig. 8a-c indicates that the addition of Aspirin greatly retards the corrosion rate of mild

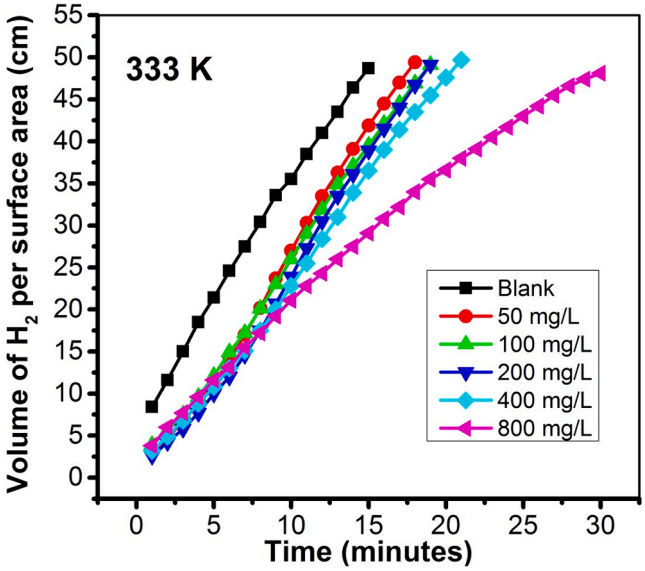

Fig. 7. Variation of volume of hydrogen evolved (V_H) with time for the mild steel coupons in 1 M H_2SO_4 solutions containing Aspirin at 333 K.

Table 3
Calculated corrosion rate, surface coverage and inhibition efficiency of mild steel in 1 M H_2SO_4 in the presence and absence of Aspirin.

	Corrosion rate (cm/min)				Surface coverage (θ)				Inhibitor efficiency (%IE)			
Conc.	303 K	313 K	323 K	333 K	303 K	313 K	323 K	333 K	303 K	313 K	323 K	333 K
Blank	0.0423	0.0736	0.1193	0.1667								
50 mg/L	0.0309	0.0584	0.1072	0.1681	0.2695	0.2065	0.1014	−0.008	26.9	20.7	10.1	−0.8
100 mg/L	0.0196	0.0547	0.0953	0.153	0.5366	0.2567	0.2012	0.0822	53.6	25.7	20.1	8.2
200 mg/L	0.0152	0.0536	0.0873	0.159	0.6406	0.2717	0.2682	0.0462	64.1	27.2	26.8	4.6
400 mg/L	0.0122	0.0306	0.0751	0.1418	0.7115	0.5842	0.3705	0.1494	71.2	58.4	37.1	14.9
800 mg/L	0.0088	0.0273	0.0536	0.0899	0.7919	0.6290	0.5507	0.4607	79.2	62.9	55.1	46.1

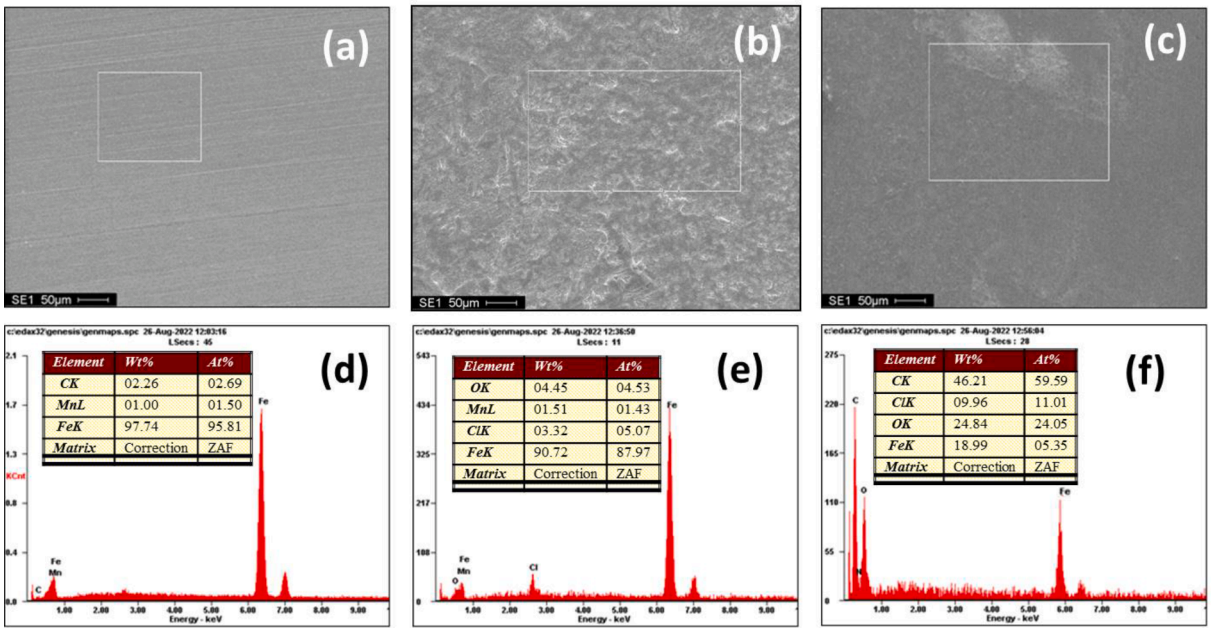

Fig. 8. SEM images and EDS spectra for mild steel surfaces: (a) & (d) polished surface, (b) & (e) without aspirin (c) & (f) with 800 mg/L Aspirin extract in 1 M H_2SO_4 solution for 1 h at 303 K.

steel in H_2SO_4 solutions.

Fig. 8 d–f shows the EDX spectra and corresponding percentage weight contents of the constituent elements. Fig. 8d is the EDX spectrum of polished mild steel which indicates characteristic peaks of Fe (97.74 wt%). Fig. 8e is the EDX spectrum of mild steel after exposure to 1.0 M H_2SO_4 in the absence of Aspirin; which indicates a drop in wt% of Fe to 90.72 wt% accompanied with peaks for O (4.45 wt%), Cl (3.32 wt%) and minor element Mo (1.51 wt%). This suggests the formation of a corrosion layer which is responsible for the decrease in the intensity of the Fe peak and the pronouncement of O and Cl. Fig. 8f shows the mild steel surface after exposure to 1.0 M H_2SO_4 in the presence of 800 mg/L. The Fe content is seen to drop drastically to 18.89 wt% while the O content increased to 24.84 wt% with the appearance of a pronounced carbon signal of 46.21 wt% alongside Cl (9.96 wt%). This indicates the formation of a barrier layer of corrosion film which is believed to be composed of adsorbed molecules of Aspirin. Fig. 8 indicates that the presence of Aspirin inhibits the corrosion of mild steel in 1 M H_2SO_4.

Thermodynamic parameters

Thermodynamic parameters such as the activation energy (E_a), enthalpy (ΔH°) and entropy of activation (ΔS°) were calculated from the temperature-dependent corrosion rate so as to gain more insights into the nature of interaction of Aspirin with the mild steel surface. The activation energy was calculated using the Arrhenius equation (equation (3)) while the transition state equation (equation (4)) was used to calculate the enthalpy (ΔH_{ads}), and entropy (ΔS_{ads}) [19–21].

$$\ln C_R = lnA - \frac{E_a}{RT} \tag{3}$$

$$\left(\frac{CR}{T}\right) = \ln\frac{K}{h} + \frac{\Delta S}{R} + -\frac{\Delta H}{RT} \tag{4}$$

where C_R is the rate of corrosion, E_a is the apparent activation energy, R is the universal gas constant, T is the absolute temperature, and A is the frequency factor.

The Arrhenius plot of the corrosion of mild steel in the absence and presence of Aspirin is shown in Fig. 9. The activation energy was calculated from the slope ($-E_a/2.303R$) of the trend line of the Arrhenius plot and the values obtained are listed in Table 4. The transition state plot of the corrosion of mild steel in the absence and presence of Aspirin is shown in Fig. 10. The enthalpy of activation (ΔH^o) and the entropy of activation (ΔS^o) for the corrosion of mild steel in 1 M H_2SO_4 were calculated from the slope and intercept transition state equation, respectively and the values are listed in Table 4. The calculated values of E_a were higher in the presence of the inhibitors (47.5 kJ/mol–73.3 kJ/mol) compared to the blank solution (32.0 kJ/mol). This suggests that the Aspirin molecules are physically adsorbed on the mild steel surface. Physical adsorption occurs due to the electrostatic force between the metal surface and Aspirin molecules [16,17]. The values of the standard entropy of activation (ΔS^o) in the absence and presence of Aspirin were all positive. This can be interpreted to mean that the activated complex in the rate determining step represents dissociation rather than association step, implying that during the adsorption process, an increase in the degree of orderliness takes place when moving to the activated complex from the reactants. The positive values of entropy also indicate

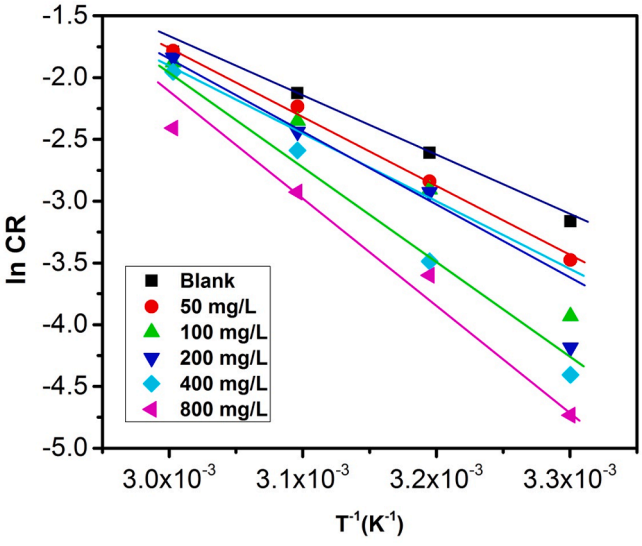

Fig. 9. Arrhenius plot for the corrosion of mild steel in 1 M H_2SO_4 solution in the presence and absence of Aspirin.

Table 4
Thermodynamic parameters for the corrosion of mild steel in the presence and absence of inhibitor.

Conc. (mg/L)	ΔH (kJ/mol)	ΔS (kJ/mol)	E_a (kJ/mol)
Blank	35.6	1148.4	38.2
50	70.7	150.8	73.3
100	66.7	1242.5	69.3
200	61.7	1227.4	64.3
400	44.8	117.2	47.5
800	40.9	1158.7	24.5

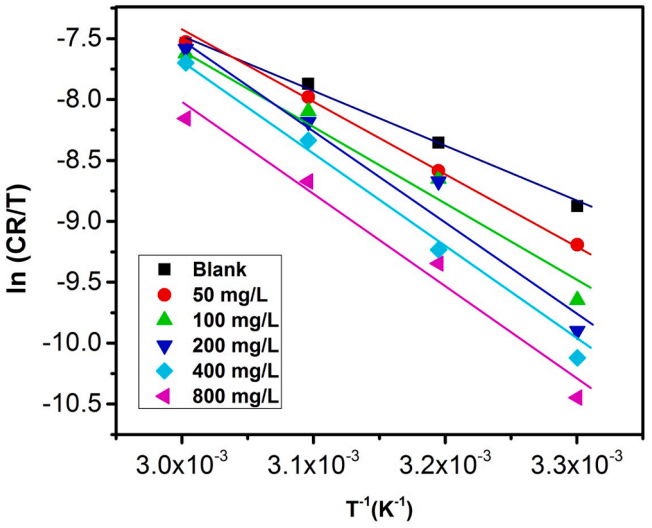

Fig. 10. Transition state plots for mild steel in 1 M H_2SO_4 solution in the presence and absence of Aspirin.

that the process is spontaneous [16].The values of the enthalpy of activation (ΔH^o) in the presence and absence of inhibitor are all positive. The positive sign of ΔH^o is associated with an endothermic nature of the corrosion process. The greater values in the presence of the inhibitor suggest that more energy needs to be supplied to the system to drive the corrosion process; this is in line with the notion that a protective barrier has been formed on the mild steel surface.

Adsorption consideration

The experimental data was further tested with three different adsorption isotherms in order to acquire more information on the nature of interaction between Aspirin and the mild steel surface. The isotherms tested are Langmuir, Freundlich and Temkin adsorption isotherms. The linear regression coefficient (R^2) was used to adjudge the model that best fit the experimental values. The experimental data was tested for its consistency with Langmuir theory which is represented by equation (5) [6,7].

$$\frac{c}{\theta} = \frac{1}{K_{ads}} + c \tag{5}$$

where c is the Aspirin concentration, θ is the degree of surface coverage and K_{ads} is the adsorption – desorption equilibrium constant. The values of K_{ads} were calculated and presented in Table 5. The value of K_{ads} denotes the strength between the adsorbate and adsorbent, large values of K_{ads} imply more efficient adsorption and hence better inhibition efficiency [17]. Table 5 indicates that the K_{ads} values decrease with temperature rise suggesting that the interaction between the inhibitor molecules and the mild steel surface becomes weaker with temperature rise. This indicates that the inhibitor molecules are physically adsorbed onto the mild steel surface. The values for the free energy of adsorption ΔG_{ads} were calculated from equation (6) [5–7].

Table 5
Equilibrium constant (K_{ads}), Adsorption free energy (ΔG_{ads}) and Correlation factor (R^2) deduced from Langmuir, Temkin and Freundlich isotherms for the corrosion of mild steel in 1 M H_2SO_4 inhibitors at different temperature.

Isotherm	Temp (K)	K_{ads}	ΔG_{ads} (KJ /mol)	R^2
Langmuir	303	0.2216	−6.3	0.8825
	313	0.0035	−4.2	0.9016
	323	0.0013	−6.9	0.7715
	333	0.0004	−10.4	0.6161
Temkin	303	13.7	−16.7	0.7543
	313	12.6	−17	0.8578
	323	11.9	−17.4	0.5782
	333	12.9	−18.2	0.5558
Freundlich	303	0.56	−8.7	0.4179
	313	1.77	−11.9	0.2003
	323	1.19	−11.2	0.0184
	333	3.93	−14.9	0.5133

$$\Delta G_{ads} = -RT\ln(K_{ads} \times 55.5) \tag{6}$$

where ΔG_{ads} is the free energy of adsorption, K_{ads} is the adsorption–desorption equilibrium constant, R the universal gas constant and T the temperature. The calculated results of ΔG_{ads} are presented in Table 5. The negative values of ΔG_{ads} indicate spontaneity and stability of the adsorption layer [23,24]. The experimental data were also tested using Temkin and Freundlich isotherms which are expressed in equations (7) and (8), respectively. The parameters deduced from Langmuir, Fruendlich and Temkin isotherms are presented in Table 5.

$$\theta = \frac{RT}{b}\ln K + \frac{RT}{b}\ln c \tag{7}$$

$$\log\theta = \log K_f + \frac{1}{n}\log c \tag{8}$$

where R is the universal gas constant, θ is the surface coverage, c is the concentration of inhibitor, b Temkin constant, K_{ads} adsorption–desorption equilibrium constant, f is the heterogeneous factor and T is the temperature. From Table 5, the R^2 values obtained from the plots at different temperature are generally seen to deviate from unity. The values R2 obtained from Langmuir isotherm showed the least deviation from unity. The deviation of the correlation factor from unity shows that the Langmuir isotherm is more suitable compared to the Temkin and Fruendlich isotherms for describing the adsorption behavior of Aspirin on the mild steel surface.

The Gibbs free energy of adsorption ΔG^o_{ads} was calculated from equation (6) and the values obtained are listed in Tables 5. The ΔG^o_{ads} values ranged from −4.2 to −18.2 kJ mol^{-1}. These values of ΔG^o_{ads} are > -20 kJ mol^{-1} and indicate that the acetylsalicylic molecules are physically adsorbed as a result of electrostatic forces of attraction [17]. On the other hand, values of ΔG^o_{ads} < -20 kJ mol^{-1} or less is considered to be as result of chemical adsorption which involves the transfer or sharing of charge from the inhibitor to the surface of metal to form a kind of co-ordinate bond [22].

The adsorption–desorption equilibrium constant K_{ads} obtained from the Langmuir isotherms decreased from 0.2216 to 0.0004 with the increase in temperature from 303 K to 313 K. This indicates that the acetylsalicylic moles are getting more weakly adsorbed with rise in temperature which is consistent the proposed physisorption mechanism.

Kinetics of the corrosion process: Rate constant and half – Life

The corrosion reaction is a heterogeneous reaction which is composed of anodic and cathodic reactions at the same or different rate. The experimental data was tested for its consistency with the integrated first and second order reaction kinetics equation given by equation (9) and (10).

$$k_1 = \frac{2.303}{t} log(V/V_\infty) \quad (9)$$

$$k_2 = \frac{1}{t} \times \frac{V}{V_\infty (V_\infty - V)} \quad (10)$$

where V is the volume of H_2 evolved (cm^3), $V\infty$ is the volume of hydrogen evolved at the end of the corrosion test k_1 is the first order rate constant in (min), k_2 is the second order rate constant and t is the immersion time in [12,13]. The rate constant at different temperature and concentration of blank, 400 mg/L and 800 mg/L are tabulated in Table 6. The consistency of the experimental data with the first and second order reaction kinetics were adjudged from the value of the rate constant which is expected not to vary significantly irrespective of concentration at a particular temperature (The values of k should be approximately equal across the concentrations tested). The blank solution, 400 mg/L and 800 mg/L of Aspirin were used for the kinetic evaluation of the corrosion rate. The experimental data were found to be consistent with the first order reaction kinetics at lower temperatures (303 K and 313 K) and thereafter transit to second order rate kinetics at higher temperature (323 K and 333 K). The values of k_1 were found to be approximately equal across the concentrations tested including the blank solution. It is also observed that half-life of mild steel increased with Aspirin concentration.

Computational details

Optimization and quantum chemical parameters

The computational details and quantum chemical calculation were to obtain more information on the molecular properties of Aspirin and the probable adsorption mode in the mild steel surface. The computational parameters of Aspirin was studied by B3LYP method / 6–31 + G (d,p) basis sets in the gaseous phase. Quantum calculations were used to obtain the energy values of highest occupied molecular orbital (HOMO) and lowest unoccupied molecular orbital (LUMO) from which the ionization energy (IP) and electronic affinity (EA), chemical hardness (X), band gap (ΔE), softness (σ) and electronegativity (η) were calculated using equation 11–16 [49–56].

$$\mathbf{IP} = -\mathbf{E_{HOMO}} \quad (11)$$

$$\mathbf{EA} = -\mathbf{E_{LUMO}} \quad (12)$$

$$\mathbf{X} = \frac{\mathbf{IP} - \mathbf{EA}}{2} \quad (13)$$

$$\eta = \frac{\mathbf{IP} + \mathbf{EA}}{2} \quad (14)$$

Table 6
Kinetic parameters of the corrosion of mild steel in the presence of Aspirin: rate constant.

Temp (K)	Conc. (mg/L)	Rate constant
	Blank	0.058
303	400	0.063
	800	0.062
	Blank	0.067
313	400	0.059
	800	0.072
323	Blank	0.762
	400	0.791
	800	0.733
333	Blank	1.681
	400	1.647
	800	1.850

$$\sigma = \frac{1}{\eta} \quad (15)$$

$$\Delta E = LUMO - HOMO \quad (16)$$

The distribution of electron density structure in the frontier molecular orbitals (FMO) i.e. HOMO and LUMO of Aspirin is shown in Fig. 11. The HOMO distribution of electrons over the Aspirin molecule shows the potential participation of molecule in the possible donation of the electron to the vacant Fe orbital of the metal surface which results in the adsorption of Aspirin on the metal by the formation of a coordinate bond through the lone pairs on the Aspirin molecule. On the other hand, LUMO distribution of electrons over the inhibitor molecule shows that it can also accept the electron from the Fe orbital of metal and hence shows possible donor–acceptor behavior relationship with the metal surface metal surface [57,58].

The calculated values for E_{HOMO}, E_{LUMO}, ΔE, μ, IP, EA are −7.33 eV, −2.06 eV, 5.27 eV, 5.79 eV, 7.33 eV and 2.06 eV, respectively. The higher the value of $\mathbf{E_{HOMO}}$, the higher electron donation tendency whereas the lower the value of $\mathbf{E_{LUMO}}$ the higher electron receptor tendency. The reactivity of Aspirin was determined by the $\Delta\mathbf{E}(\mathbf{E_{HOMO}} - \mathbf{E_{LUMO}})$, high value of $\Delta\mathbf{E}$ represent high reactivity of the molecule with metal that results in the observed inhibitory effect [59]. Dipole moment is also another important structural index, it is widely reported that small value of dipole moment favor the accumulation of inhibitor molecules on the surface of steel, thereby enhancing the inhibition efficiency of the inhibitor molecules on the surface of the metal. In the presence of acids as in the present case, the Aspirin molecule is protonated which facilitates its adsorption on the steel surface. The frontier molecular orbital energies are used as reactivity indices. The calculated values of the E_{HOMO} and E_{LUMO}, dipole moment, ionization energy and electron affinity are within the range of values reported for effective corrosion inhibitors elsewhere [39,56–59].

Fukui functions

The analysis of Fukui indices provides useful data about the local reactivity of a compound. By using the information obtained from Fukui functions, we can determine the atoms in a molecule with a higher tendency to accept and loose electrons [39]. The Fukui functions obtained for Aspirin are shown in Table S1 of the supplementary materials. The nucleophilic sites f_k^-, electrophilic sites f_k^+ and the dual descriptor $\Delta f_{(K)}$ were calculated using the Milliken population analysis (equation 17–19).

$$f_k^+ = q(N+1) - -q(N) \quad (17)$$

$$f_k^- = q(N) - -q(N-1) \quad (18)$$

$$f_{(k)} = f_k^+ - f_k^- \quad (19)$$

where q_k is the atomic charge in its neutral (N), cationic (N-1) or anionic (N + 1) state. The outcome Fukui data for Aspirin are shown in Table S1.

The atom that possesses the highest value of (f_k^-) is the oxygen (15)O atom attached directly to the aromatic ring with value of 0.1058, this indicates its high ability to donate electron to the mild steel surface. The carbon atom C(1) of aromatic moiety also possesses high value of (f_k^-) (0.1111) and participates in the donating process. Using the dual descriptor ($\Delta f_{(k)}$), we can obtain two indications; for donor sites $\Delta f_{(r)} < 0$ and acceptor sites $\Delta f_{(r)} > 0$. Our data indicate that for the donor sites, the oxygen atom (15)O is the best with value of −0.0470 for Aspirin. On the other hand, (11)C is the best acceptor sites for Aspirin with a value of 0.0836 [39,55–59].

Natural bonding orbital's (NBO)

The natural bond orbital (NBO) analysis transforms molecular orbital wave function into one center (lone pair) and two center bond repre-

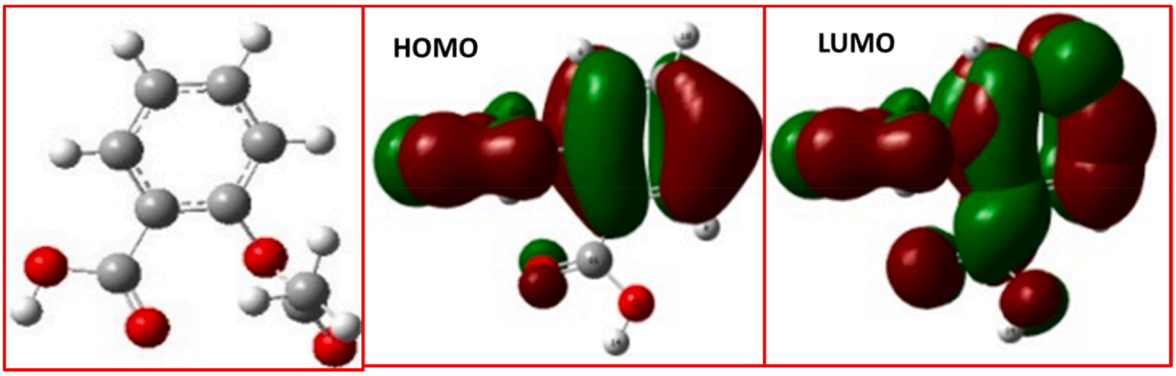

Fig. 11. Optimized structure, HUMO and LUMO of Aspirin molecule.

sentation. This kind of categorization gives an appealing chemical representation since it highlights the individual bonds and lone pairs that play a role in the chemical process. The diagonal elements of the Fock matrix in an NBO analysis represent the energies of localized bonds σ* and lone pair of electrons, while the off – diagonal elements represent bond -σ* and normally small σ* to σ interactions. The larger the $E^{(2)}$ values the more intensive is the interaction between electron donor to electron acceptor and the greater the extent of conjugation of the whole system. Delocalization of electron density between occupied Lewis-typed (bond or lone pair) NBO orbital's and formally unoccupied (antibond or Rydberg) non-Lewis NBO orbital's corresponds to a stabilizing donor – acceptor interactions for each donor NBO (i) and acceptor NBO (j), the stabilization energy $E^{(2)}$ associated with electron delocalization between donor and acceptor is estimated using equation (20).

$$E^{(2)} = q_i \frac{F_{ij}^2}{E_{j-E_i}} \tag{20}$$

where q_i is the donor orbital occupancy, E_i, E_j are diagonal elements (orbital energies) and F_{ij} is the off-diagonal NBO Fock matrix element [47,48]. The results of second order perturbation analysis of the Fock matrix at B3LYP/6–31 + G (d,p) basic set, level of theory are presented in Table S2 of supplementary material. NBO analysis revealed that the π (C5-C6) to π* (C3– C4) interaction give the strongest stabilization to the system with a stabilization energy of 23.57 kcal/mol.

Molecular dynamics simulation studies

Molecular dynamic simulations were carried out and the experimental conditions were imposed on the system to obtain the equilibrium adsorption of Aspirin on Fe (1 1 0) surface at 303 K, 313 K, 323 K and 333 K. Fig. 12 shows the top and side view of various adsorption configuration at the temperature and energy variation obtained from molecular dynamic simulation for inhibitor at 303–333 K. Results showed that the inhibitor molecules which were adsorbed on the metal surface assumed a flat configuration which obviously enhanced the surface coverage of Aspirin molecules over the metal surface which leads to inhibition of corrosion. The binding energies obtained from the molecular dynamic simulation are represented in Table 7. A high negative $E_{binding}$ shows the greater binding of inhibitor with metal and leads to a higher value of $E_{Binding}$ which results in greater inhibition efficiency. The computed interaction energies at different temperature are shown in Table 7 and the maximum was at 323 K with a value of −119.11 kcal/mol. Fig. 13 shows the schematic representation of corrosion mechanism depicting the mode of adsorption of aspirin molecules on the mild steel substrate through the oxygen hetero atoms.

Comparative studies of the studied inhibitor with previous drug based inhibitors

Table 8 present the comparison of the inhibitory performance of aspirin with previously studied drugs. The maximum inhibition

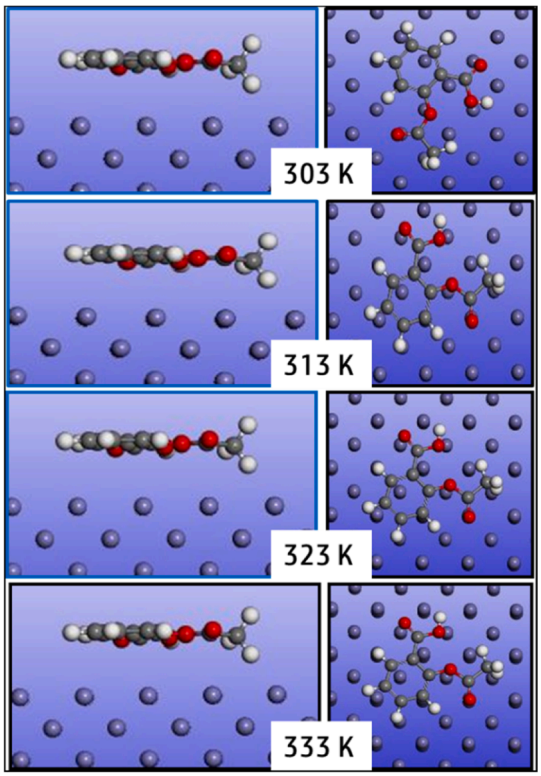

Fig. 12. Side and top view of the equilibrium adsorption configuration of the inhibitor on the Fe (1 1 0) surface at different temperatures.

Table 7
Total binding energies of Aspirin on mild steel at different temperatures.

T/K	$E_{binding}$/(kcal/mol)
303 K	−119.071
313 K	−119.110
323 K	−117.147
333 K	−119.069

efficiency recorded at different electrolyte/ inhibitor combinations for Losartan, Dexamethasone, Rosuvastatin, Dapsone, Lidocaine, Amodiaquine, Ketoconazole, Pyridil, and Neomycin are 80 %, 92 %, 90 %, 95 %, 76 %, 44 %, 46 %, 71 %, and 76 %, respectively. It is seen the corrosion inhibition performance of aspirin with an efficiency of 79 % compared competitively with other drugs in the literatures given the aggressive 1.0 M H_2SO_4 medium used.

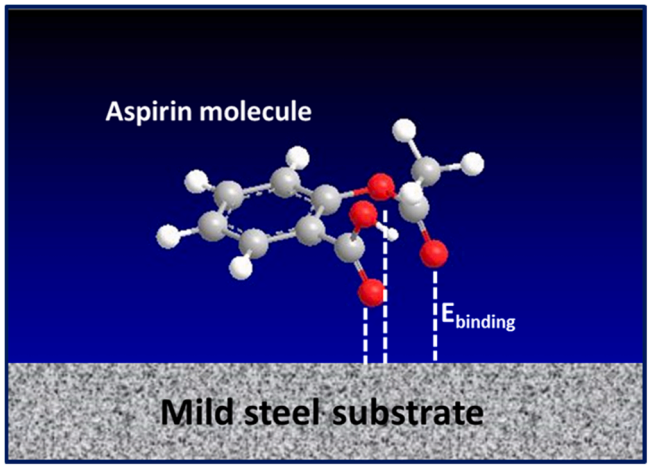

Fig. 13. Schematic representation of corrosion mechanism depicting the mode of adsorption of Aspirin molecules on the mild steel substrate.

Table 8
Comparative studies of Aspirin with other similar drug-based inhibitors.

Drug	Electrolyte	Max Conc. (mg/L)	IE (%)	Ref
Losartan	2.0 M HCl	400	80	[60]
Dexamethasone	1.0 M HCl	1963	92	[61]
Rosuvastatin	0.5 M H_2SO_4	600	90	[62]
Dapsone	0.5 M H_2SO_4	496	95	[63]
Lidocaine	1.0 M HCl	300	76	[64]
Amodiaquine	0.1 M HCl	2135	44	[65]
Ketoconazole	0.1 M H_2SO_4	50	46	[66]
2,21 –Pyridil	0.5 M HCl	106	71	[67]
Neomycin	1.0 M H_2SO_4	553	76	[68]
Aspirin	1.0 M H_2SO_4	800	79	This paper

The present report indicate that aspirin is a possible alternative to the widely applied toxic corrosion inhibitors in the industry, however, there is need for the expansion of the scope of this current study to capture the nature and properties of the adsorbed aspirin molecules on the metal surface in order to gain a complete understanding of its corrosion inhibition mechanism. Specially, an additional advantage of aspirin over other drugs its cost effectiveness and facile synthetic route making its application on an industrial scale more practicable.

Conclusion

The corrosion inhibition potential of Aspirin has been evaluated using a combined theoretical and experimental approach. The results show that Aspirin inhibits the corrosion of mild steel in H_2SO_4 solution. The inhibition efficiency of the drug increased with increase in concentration and decreased with the rise in temperature. The optimum condition for the inhibition efficiency of 79.1 % was at 800 mg/L at 333 K. The inhibitive action of Aspirin is as a result of physical adsorption of its molecules on the surface of mild steel. The presence of Aspirin increases the corrosion activation energy. Kinetics studies revealed that the corrosion follows a first order reaction kinetics at lower temperatures and second order kinetics at higher temperatures. Thermodynamic considerations revealed that the activation energy is increases in the presence of Aspirin when compared with that of the free solution, the enthalpy of activation indicate that the corrosion process predominantly endothermic, the entropy of activation shows that the process is spontaneous. DFT and quantum chemical calculation revealed a very strong interaction between the Aspirin molecules and the mild steel surface and the stable adsorption configurations were obtained through molecular dynamics stimulation. The present report indicate that aspirin is a possible alternative to the widely applied toxic corrosion inhibitors in the industry, however, there is need for the expansion of the scope of this current study to capture the nature and properties of the adsorbed aspirin molecules on the metal surface in order to gain a complete understanding of its corrosion inhibition mechanism.

CRediT authorship contribution statement

Alexander I. Ikeuba: Conceptualization, Formal analysis, Investigation, Writing – review & editing. **Omang B. John:** Investigation, Resources, Writing – review & editing. **Victoria M. Bassey:** Resources, Writing – review & editing. **Hitler Louis:** Resources, Writing – review & editing. **Augustine U. Agobi:** Resources, Writing – review & editing. **Joseph E. Ntibi:** Resources, Writing – review & editing. **Fredrick C. Asogwa:** Writing – review & editing.

Declaration of Competing Interest

The authors declare that they have no known competing financial interests or personal relationships that could have appeared to influence the work reported in this paper.

Data availability

Data will be made available on request.

Appendix A. Supplementary data

Supplementary data to this article can be found online at https://doi.org/10.1016/j.rechem.2022.100543.

References

[1] R. Wang, H. Nagano, Y. Ling, Ling Y Corrosion behaviour of mild steel in chloride solutions with Na2HPO4 additive and the development of antifreeze, Corros. Eng., Sci. Technol. 53 (sup1) (2018) 67–74.
[2] Nwokolo IK, Shi H, Ikeuba AI, Gao N, Li J, Ahmed S, Liu F, Synthesis, Characterization and Investigation of Anticorrosion Properties of an Innovative Metal–Organic Framework, ZnMOF-BTA, on Carbon Steel in HCl Solution.
[3] A.I. Obike, K.J. Uwakwe, E.K. Abraham, A.I. Ikeuba, W. Emori, Review of the losses and devastation caused by corrosion in the Nigeria oil industry for over 30 years, Int. J. Corros. Scale Inhibition. 1 (2020) 74–91.
[4] I.E. Uwah, B.U. Ugi, P.C. Okafor, A.I. Ikeuba, Investigation of the corrosion inhibition effects of bitters on mild steel in acidic media: A case study of Andrographis paniculata and Vernonia amygdalina, Int. J. Appl. Chem. 9 (2013) 73–88.
[5] R.G. Sundaram, G. Vengatesh, M. Sundaravadivelu, Surface morphological and quantum chemical studies of some expired drug molecules as potential corrosion inhibitors for mild steel in chloride medium, Surf. Interfaces 22 (2021) 100841.
[6] S. Tanwer, S.K. Shukla, Recent advances in the applicability of drugs as corrosion inhibitor on metal surface: A review, Curr. Res. Green Sustain. Chem. 5 (2022) 100227.
[7] K. Zakaria, M.A. Abbas, M.A. Bedair, Herbal expired drug bearing glycosides and polysaccharides moieties as green and cost-effective oilfield corrosion inhibitor: Electrochemical and computational studies, J. Mol. Liq. 352 (2022) 118689.
[8] P. Okafor, E. Ebenso, Inhibitive action of Carica Papaya extracts on the corrosion of mild steel in acidic media and their adsorption characteristics", Pigm. Resin Technol. 36 (2007) 134–140.
[9] I.E. Uwah, B.U. Ugi, P.C. Okafor, A.I. Ikeuba, Investigation of the corrosion i I. E. nhibition effects of bitters on mild steel in acidic media: A case study of Andrographis paniculata and Vernonia amygdalina, Int. J. Appl. Chem. 9 (1) (2013) 73–88.
[10] P.C. Okafor, M.E. Ikpi, I.E. Uwah, E.E. Ebenso, U.J. Ekpe, S.A. Umoren, Inhibitory action of phyllanthus amarus extracts on the corrosion of mild steel in acidic media, Corros. Sci. 50 (8) (2008) 2310–2317.
[11] P.C. Okafor, E.E. Ebenso, U.J. Ekpe, Azadirachta indica extracts as corrosion inhibitor for mild steel in acid medium, Int. J. Electrochem. Sci. 5 (2010) 978–993.
[12] S.S. Shivakumar, K.N. Mohana, Ziziphus mauritiana leaves extract as corrosion inhibitor for mild steel in sulphuric acid and hydrochloric acid solution, Europ. J. Chem. 3 (2012) 426–432.
[13] I.B. Obot, N.O. Obi-Egbedi, Ginseng Root.A new Efficient and Effective Eco-Friendly Corrosion Inhibitor for Aluminium Alloy of type AA 1060 in Hydrochloric Acid Solution, Int. J. Electrochem. Sci. 4 (1277) (2010).
[14] M. Norzila, S.I. Anis, Thermodynamic Study of Corrosion Inhibition of Mild Steel in Corrosive Medium by Piper nigrum Extract, Ind. J. Sci. Technol. 17 (2015) 1–6.
[15] C. Sudhakar, M. Saravanabhavan, K.S. Ramesh, V.N. Badavath, S. Chandrasekar, B. Babu, M. Sekar, Pharmacological and quantum chemical studies of 2

aminobenzo[d]thiazol-3-ium 4-chlorobenzenesulphonate: Synthesis, spectral, thermal analysis and structural elucidation, Resul. Chem. 4 (2022) 100442.
[16] A. Singh, A. Kumar, T. Pramanik, theoretical approach to the study of some plant extracts as green corrosion inhibitor for mild steel in HCl solution, Orient. J. Chem. 29 (1) (2013) 277–283.
[17] A.I. Ikeuba, P.C. Okafor, Green corrosion protection for mild steel in acidic media: Saponins and crude extracts of Gongronema latifolium, Pigm. Resin Technol. 48 (2018) 57–64.
[18] A.I. Ikeuba, B.I. Ita, P.C. Okafor, V.M. Bassey, B.U. Ugi, E.B. Kporokpo, Green Corrosion Inhibitors for Mild Steel in H2SO4 Solution: Flavonoids of Gongronema latifolium, J. Protect. Metal. Phys. Chem. Surf. 51 (2015) 1043–1049.
[19] A.I. Ikeuba, P.C. Okafor, U.J. Ekpe, E.E. Ebenso, Alkaloid and non-alkaloid ethanolic extracts from seeds of Garcinia kola as green corrosion inhibitors of mild steel in H2SO4 solution, Int. J. Electrochem. Sci. 8 (2013) 7455–7467.
[20] F.E. Abeng, M.E. Ikpi, P.C. Okafor, V.C. Anadebe, K.J. Uwakwe, A.I. Ikeuba, N. A. Okafor, Corrosion inhibition of API 5L X-52 steel in oilfield acidizing solution by Gentamicine and sulfamethoxazole: Experimental, plane-wave density functional theory (PWDFT) and the generalized-gradient approximation (GGA) simulations, J. Adhes. Sci. Technol. (2021), https://doi.org/10.1080/01694243.2021.2013591.
[21] D. Wang, B. Xiang, Y. Liang, S. Song, C. Liu, Corrosion control of copper in 3.5 wt. % NaCl solution by domperidone: experimental and theoretical study, Corros. Sci. 85 (2014) 77–86.
[22] P. Geethamani, P. Kasthuri, S. Aejitha, Corrosion inhibition of mild steel in sulphuric acid medium by Ambroxol drug, J. Appl. Chem. Sci. Int. 4 (2015) 151–157.
[23] A.K. Singh, M.A. Quaraisha, Effect of Cefazolin on the corrosion of mild steel in hydrochloric acid solution, Open Electrochem. J. 52 (2010) 152–160.
[24] S.S. Amaal, O.A. Entesar, Synthesis characterization of new polytriazole derivative from 26] and theoretical with corrosion inhibitor study for stainless steel in acidic medium, Res. J. Pharm. Technol. 14 (2021) 3721–3726.
[25] N.O. Eddy, S.A. Odoemelan, P. Ekwumemgbo, Inhibition of the corrosion of mild steel in H_2SO_4 by penicillin G, Scient. Res. Essays. 4 (2009) 33–38.
[26] A.S. Fouda, K. Shalabi, Moxifloxacin antibiotic as green corrosion inhibitor for carbon steel in 1 M HCl, J. Bio Tribo Corros. 2 (2016) 1–3.
[27] U. Bishir, M. Hasmerya, H.A. Hassan, A. Madzlan, Inhibition performance of mild steel corrosion in acidic media using 2- Thiophene acetyl chloride, Bayero J. Pure Appl. Sci. 10 (2017) 590–595.
[28] M. Alfakeer, M. Abdallah, A. Fawz, Corrosion inhibition effect of expired ampicillin and flucloxacillin drugs for mild steel in aqueous acidic medium, Int. J. Electrochem. Sci. 15 (2020) 3283–3297.
[29] I.B. Obot, N.O. Obi-Egbedi, S.A. Umoren, E.E. Ebenso, Adsorption and kinetic studies on the inhibition potential of fluconazole for the corrosion of AL in HCL solution, Chem. Eng. Commun. 198 (5) (2011) 711–725.
[30] A.A. Abdel-Azim, R. Milad, R. El-Ghazawy, Corrosion inhibition efficiency of water soluble ethoylatedrimethyl propane by gravimetric analysis, Egypt. J. Petrol. 23 (2014) 15–20.
[31] M.S. Nooshabadi, M.S. Ghandchi, Introducing the santolina chamaecyparissus extract as a suitable green inhibitor for 304 stainless steel corrosion in strong acidic medium, Metallurg. Mater. Transacions. *A*. 46 (2015) 5139–5148.
[32] A.I. Ikeuba, B. Zhang, J. Wang, E.H. Han, W. Ke, Electrochemical, TOF-SIMS and XPS studies on the corrosion behavior of the Q-phase, Appl. Surf. Sci. 490 (2019) 535–545.
[33] A.I. Ikeuba, F. Kou, H. Duan, B. Zhang, J. Wang, E.H. Han, W. Ke, Understanding the Electrochemical behavior of MgZn2 as a function of pH, J. Solid State Electrochem. 23 (2019) 1165–1177.
[34] Y. Ting, Z. Shengtao, F. Li, Investigation of imidazole derivatives as corrosion inhibitors of copper in sulfuric acid: combination of experimental and theoretical research, J. Taiwan Instit. Chem. Eng. 106 (2020) 118–129.
[35] Z. Rouifi, F. Benhiba, M.E. Faydy, T. Laabaissi, H. About, H. Oudda, I. Warad, A. Guenbour, B. Lakhrissi, A. Zarrouk, Performance and computational studies of new soluble triazole as corrosion inhibitor for carbon steel in HCl, Chem. Data Collection. 22 (2019) 100242.
[36] Essien UB, Ikpi ME, Ikeuba AI, Essien NB. Experimental and Computational Chemistry investigations of tartaric acid as green corrosion inhibitor for API 5L X 52 carbon steel in 0.5 M HCl. Commun. Phys. Sci. 2021; 7:482-193.
[37] K. Khaled, Molecular simulation, quantum chemical calculations and electrochemical studies of inhibition of mild steel by triazoles, Electrochem. Acta. 53 (2008) 3484–3492.
[38] T. Mouheddin, A.U. Alhaffar, B.O. Ime, A.A. Shaikh, Isoxazolidine derivatives as corrosion inhibitors for low carbon steel in HCl solution: experimental, theoretical and effect of KI studies, Roy. Soc. Chem. 8 (2018) 1764–1776.
[39] S.T. Udaya, S. Karsten, P.N. Eliano, J. Young-Hoon, K. Jacek, P.B. Kevin, A.G. Paul, Aspirin as an Adjunctive Pharmacologic Therapy Option for COVID-19: Anti-Inflammatory, Antithrombotic, and Antiviral Effects All in One Agent, J. Exp. Pharmacol. 13 (2021) 957–970.
[40] W. Xie, Y. Luo, X. Liang, Z. Lin, Z. Wang, M. Liu, The Efficacy and Safety Of Aspirin As The Primary Prevention Of Cardiovascular Disease: An Updated Meta-Analysis, Ther. Clin. Risk Manag. 15 (2019) 1129–1140.
[41] E.F. Olasehinde, S.J. Olusegun, A.S. Adesina, S.A. Omogbehin, H. Momoh-Yahayah, Inhibitory action of Nicotiana tobacum extracts on the corrosion of mild steel in HCl: adsorption and thermodynamic study, Nature. Science. 11 (2013) 83–90.
[42] D. Thirumoolan, V.A. Katkar, G. Gunasekaran, T. Kanai, K. Anver Basha, Hyperbranched poly(cyanurateamine): A new corrosion inhibitor for mild steel in hydrochloric acid medium, Prog. Org. Coat. 77 (8) (2014) 1253–1263.
[43] K.O. Shamsheera, R.P. Anupama, J. Abraham, Computational simulation, surface characterization, adsorption studies and electrochemical investigation on the interaction of guar gum with mild steel in HCl environment, Results in Chemistry. 2 (2020) 100054.
[44] K.M. Bobby, M. Rahuma, H. Khakbaz, R. Melchers, Antipsychotic drug waste: A potential corrosion inhibitor for mild steel in the oil and gas industry, Waste Manage. 145 (2022) 38–47.
[45] S. Pour-Ali, S. Hejazi, Tiazofurin drug as a new and non-toxic corrosion inhibitor for mild steel in HCl solution: Experimental and quantum chemical investigations, J. Mol. Liq. 354 (2022) 118886.
[46] M.A. Quraishi, A. Singh, V.K. Singh, D.K. Yadav, A.K. Singh, Green Approach to Corrosion Inhibition of Mild Steel in Hydrochloric Acid and Sulphuric Acid Solutions by the Extract of Murrayakoenigii Leaves, Mater. Chem. Phys. 122 (1) (2010) 114–122.
[47] Neese F, An Ab initio, DFT and semi empirical SCF- MO package, version 2.7.0, Max planck institute for Bioionorganic chemistry, Mulheim ander Ruhy, Germany, **2012**.
[48] S. Bashir, V. Sharma, H. Lgaz, I. Chung, A. Sigh, A. Kumar, The inhibition action of analgin on the corrosion of mild steel in acidic medium: A combined theoretical and experimental approach, J. Mol. Liq. 04 (2018) 143–158.
[49] T. Koopmans, About the assignment of wavefunction and eigenvalues to the individual electrons of an atom, Phscia. (1993:) 104–113.
[50] Agobi AU, Louis H, Ekpunobi AJ, Unimuke TO, Ikeuba AI, Pembere MS, Ozoemena CN. (2022). Theoretical investigation of the structural, optoelectronic, and the application of waste graphene oxide/polymer nanocomposite as a photosensitizer, Mater. Res. Expr., http://iopscience.iop.org/article/10.1088/2053-1591/ac73001.
[51] S.K. Saha, P. Ghosh, A. Hens, N.C. Murmu, P. Banerjee, Density functional theory and molecular dynamics simulation study on corrosion inhibition performance of mild steel by mercapto-quinoline Schiff base corrosion inhibitor, Low- Dimens. Syst. Nanostruct. 66 (2015) 332–341.
[52] A.I. Ikeuba, B.o. Zhang, J. Wang, E.-H. Han, W. Ke, P.C. Okafor, SVET and SIET Study of Galvanic Corrosion of Al/MgZn 2 in Aqueous Solutions at Different pH, J. Electrochem. Soc. 165 (3) (2018) C180–C194.
[53] Ita BI, Hitler L, Nzeata N, Ikeuba AI, Akakuru UO, Magu TO, Pigweh AI, Muyiwa MO [1]. Approximate *l*-States Solutions to the Schrodinger Equation with Manning-Rosen plus Hellmann Potential via WKB Approximation Scheme. Sri Lankan J. Phys., 19: 37-45.
[54] A.I. Ikeuba, P.C. Okafor, B.I. Ita, A.I. Obike, F.E. Abeng, A.A. Bamigbola, U. B. Essien, Insitu SVET studies on the current density distribution on dissolving of Mg, Mg2Si, Al4Cu2Mg8Si7 and MgZn2 surfaces in sodium chloride solutions, Anti-Corros. Methods Mater. (2021), https://doi.org/10.1108/ACMM-07-2021-2518.
[55] A.I. Ikeuba, B. Zhang, B.I. Ita, SVET and ToF-SIMS Studies on the Galvanic Corrosion of β-phase/Aluminum Couple in Aqueous Solutions as a Function of pH, J. Electrochem. Soc. 167 (2) (2020), 021507.
[56] F.C. Asogwa, E.C. Agwamba, H. Louis, M.C. Muozie, I. Benjamin, T.E. Gber, G. E. Mathias, A.S. Adeyinka, A.I. Ikeuba, Structural Benchmarking, Density Functional Theory Simulation, Spectroscopic Investigation and Molecular Docking of N-(1H-pyrrol-2-yl) methylene)-4-methylaniline as Castration-Resistant Prostate Cancer Chemotherapeutic Agent, Chem. Phys. Impact 5 (2022) 100091.
[57] J. Kaya, P. Banerjee, S.K. Saha, B. Tuzun, Experimental and theoretical investigation towards anti- corrosive property of glutamic acid and poly- glutamic acid for mild steel in 1 M HCl: intramolecular synergism due, Res. Chem. Intermed. 43 (2017) 4423–4444.
[58] B.I. Ita, A.I. Ikeuba, Solutions of the Dirac equation with Gravitational plus Exponential Potential, Appl. Maths 4 (10C) (2013) 1–6.
[59] A.I. Ikeuba, B.o. Zhang, J. Wang, E.-H. Han, W. Ke, Understanding the galvanic corrosion of the Q-phase/Al couple using SVET and SIET, J. Mater. Sci. Technol. 35 (7) (2019) 1444–1454.
[60] V.C. Anadebe, O.D. Onukwuli, F.E. Abeng, Electrochemical-kinetics, MD-simulation and multi-input multi output (MISO) modeling using adaptive neuro-fuzzy inference system (ANFIS) prediction for dexamethasone drug as ecofriendly corrosion inhibitor for mild steel in 2 M HCl electrolyte, J. Taiwan Instit. Chem. Eng. 115 (2020) 251–265.
[61] Qiang Y, Guo L, Li H. Fabrication of environmentally friendly losartan potassium. film for corrosion inhibition of mild steel in HCl medium. Chemical Engineering Journal. 2021; 406:126863.
[62] M.R. Gholamhosseinzadeh, H. Aghaie, M.S. Zandi, M. Giahi, Rosuvastatin drug as a green and effective inhibitor for corrosion of mild steel in HCl and H2SO4 solutions, J Mater Res Tech. 8 (6) (2019) 5314–5324.
[63] P. Singh, D.S. Chauhan, S.S. Chauhan, G. Singh, M.A. Quraishi, Chemically modified expired dapsone drug as environmentally benign corrosion inhibitor for mild steel in sulphuric acid useful for industrial pickling process, J. Mol. Liqu. 286 (2019) 110903.
[64] H. Adel Ali, A. El-Aziz, S. Fouda, S. Amal, Electrochemical behavior for corrosion protection of mild steel (MS) in 1M HCl medium by using lidocaine drug as an inhibitor, Zastita mater. 61 (2020) 286–305.
[65] A. Akpan, N.O. Offiong, Amodiaquine drug as a corrosion inhibitor for mild steelin 0.1M HCl solution, Chem. Mater. Res. 7 (2015) 149–153.
[66] I.B. Obot, N.O. Obi-Egbedi, Adsorption properties and inhibition of mild steel corrosion in sulphuric acid solution by ketoconazole: experimental and theoretical investigation, Corrosion Sci. 52 (2010) 198–204.
[67] B.I. Ita, O.E. Offiong, The inhibition of mild steel corrosion in hydrochloric acid by 2,21 -pyridil and a-pyridoin, Mater. Chem. Phys. 51 (1997) 203–210.
[68] A. Samide, G.E. Iacobescu, B. Tutunaru, R. Grecu, C. Tigae, C. Spînu, Inhibitory properties of neomycin thin film formed on carbon steel in sulfuric acid solution: electrochemical and AFM investigation, Coatings. 7 (2017) 181.